The Effect of FeO/SiO$_2$ Ratio on the Feasibility of Utilising Iron Silicate Slags as Supplementary Cementitious Materials

A Andersson[1], *J Isaksson*[2], *L Brander*[3], *A Lennartsson*[4], *Å Roos*[5], *and F Engström*[6]

1. Associate Senior Lecturer, Luleå University of Technology, Luleå, Sweden, 971 87. Email: anton.andersson@ltu.se
2. Associate Senior Lecturer, Luleå University of Technology, Luleå, Sweden, 971 87. Email: jenny.isaksson@ltu.se
3. Senior Scientist, Research Institutes of Sweden, Mölndal, Sweden, 431 53. Email: linus.brander@ri.se
4. Senior Lecturer, Luleå University of Technology, Luleå, Sweden, 971 87. Email: andreas.lennartsson@ltu.se
5. Product Manager, Boliden Smelters, Stockholm, Sweden, 101 20. Email: ake.roos@boliden.com
6. Associate Professor, Luleå University of Technology, Luleå, Sweden, 971 87. Email: fredrik.i.engstrom@ltu.se

Keywords: iron silicate slag, copper slag, supplementary cementitious material, recycling

ABSTRACT

Slags are the most voluminous solid by-products generated in pyrometallurgical operations, and, as such, finding an application for these oxidic materials is pertinent to maintaining resource efficiency. In particular, pyrometallurgical copper production is associated with high slag rates, typically ranging from 2.2 to 3.0 tons of slag per ton produced copper, which necessitates slag valorisation. A possible application for these iron silicate slags is as supplementary cementitious materials (SCMs), which effectively lowers the CO_2 emissions per ton of cementitious material. Although utilising iron silicate slags as SCMs has been studied in previous work, the scientific literature has limited data on the effect of composition on the inherent reactivity in cementitious systems. More specifically, no reports on the impact of FeO/SiO_2 ratio have been presented in previous publications. Therefore, the present study aimed to isolate this parameter in a synthetic FeO-SiO_2-Al_2O_3-CaO-MgO-Cr_2O_3 system. Since the amorphous content is a pertinent parameter for SCMs, a high-temperature confocal laser scanning microscope (HT-CLSM) was utilised to assess the crystallisation behaviour at continuous cooling conditions. Furthermore, high-temperature rheological experiments were conducted to measure the viscosities of the slags in relation to the crystallisation behaviour. The experiments showed that depolymerising the slag by increasing the FeO/SiO_2 ratio generated a less viscous slag, which showed higher tendencies for crystallisation. Furthermore, experiments assessing the inherent reactivity as an SCM showed that depolymerising the slag by increasing the FeO/SiO_2 ratio as the sole independent parameter generated an initially more reactive slag. However, replacing SiO_2 with FeO was found to negatively affect the reactivity as measured over 7 days within the tested compositional range.

INTRODUCTION

The pyrometallurgical extraction of copper is associated with slag rates in the range of 2.2 to 3.0 tons of slag per ton produced copper (Shi, Meyer and Behnood, 2008; Gabasiane et al, 2021), and this necessitates slag valorisation to ensure a resource-efficient process. Multiple external applications are reported for the recycling of copper slags, eg, sand blasting media, auxiliary to sand in cement, and various construction applications excluding cement (Al-Jabri et al, 2006; Shi, Meyer and Behnood, 2008; Murari, Siddique and Jain, 2015; Gabasiane et al, 2021; Kero Andertun et al, 2022). An attractive valorisation route for the slag is the utilisation as an SCM, which lowers the carbon dioxide emissions per ton cementitious material since the SCM requires neither calcination nor clinkering (Lothenbach, Scrivener and Hooton, 2011).

As summarised in a previous publication (Andersson et al, 2023a), several studies have been published addressing iron silicate copper slags in SCM applications, and the assessed compositions span wide ranges in the major components. For a specific slag composition, several parameters affect the reactivity of the slag as an SCM. These parameters include, eg, the amorphous content, specific surface area, and thermal history (Skibsted and Snellings, 2019). Furthermore, in addition to generating specific surface area, the milling can be operated to cause amorphisation (Feng et al, 2019a) or activation by introducing surface defects (Romero Sarcos et al, 2021; Andersson et al, 2023a), both of which improve reactivity. The review of previously studied slag compositions showed that the slags were generated using different cooling processes, amounting to different amorphous contents, and, in addition, the slags were milled to different specific surface areas and evaluated for their performance as SCMs using different methodologies (Andersson et al, 2023a). Consequently, the previous data cannot be used across studies to evaluate the compositional aspect since essential parameters are not fixed between studies. Nevertheless, research on the isolated effects of CaO content (Feng et al, 2019b) and Al_2O_3 content (Zhang et al, 2023) on the performance of iron silicate slag in SCM applications have been performed. However, no study on the implications of changing the FeO/SiO_2 ratio has been published.

Assuming that the slag composition is fixed, two main parameters affect the appropriateness of using the slag as an SCM. Firstly, the cooling process, which correlates to the degree of crystallinity of the slag and possibly the polymerisation (Stebbins, 1988). Crystalline phases are generally considered inert in SCM applications (Snellings, 2013; Kucharczyk et al, 2018; Glosser et al, 2021), which means that the cooling rate must supersede crystallisation. Secondly, the subsequent milling of the solidified slag, which determines the specific surface area, as well as the possible amorphisation (Feng et al, 2019a), or activation from introducing surface defects (Romero Sarcos et al, 2021;

Andersson et al, 2023a). Ramanathan, Tuen and Suraneni (2022) argued that the reactivity of SCMs is controlled by the surface area, extent of amorphous phases, and compositions of the amorphous phases. Consequently, to compare the effect of chemical composition, the slags require similar specific surface areas and amorphous contents.

Based on the above, the present study aimed to offer insight into the effect of FeO/SiO_2 ratio on the suitability of forming a reactive SCM. The aim was addressed using a synthetic FeO-SiO_2-CaO-Al_2O_3-MgO-Cr_2O_3 system and evaluating how the FeO/SiO_2 ratio influences the crystallisation behaviour under continuous cooling conditions and how this relates to the viscosity of the slag. Furthermore, the effect of the FeO/SiO_2 ratio on the inherent reactivity in the SCM application for slags cooled under repeatable conditions and milled to similar specific surface areas was assessed.

METHOD

Synthesis of samples

Two iron silicate slag samples in the FeO-SiO_2-CaO-Al_2O_3-MgO-Cr_2O_3 system were synthesised, and their intended compositions given in atomic percent (at per cent) are presented in Table 1. The methodology of synthesising and granulating the samples has been accounted for in detail in a previous publication (Andersson et al, 2023b), and, therefore, the present description offers a summary.

TABLE 1 – Composition of the samples included in the study [at per cent].

Sample	FeO/SiO$_2$	FeO	SiO$_2$	CaO	Al$_2$O$_3$	MgO	Cr$_2$O$_3$
A	1.25	51.2	41.0	1.2	5.0	1.5	0.08
B	2.00	61.5	30.7	1.2	5.0	1.5	0.08

The compositions in Table 1 were mixed based on the reagent grade chemicals Fe, Fe_2O_3, SiO_2, $CaCO_3$, Al_2O_3, MgO, and Cr_2O_3. Each synthetic slag was melted in an iron crucible (>99.82 % Fe), which ensures that a partial pressure of oxygen relevant to iron silicate slags undergoing the zinc fuming process is attained (Andersson et al, 2023b). Figure 1 illustrates the graphite resistance-heated furnace employed in the experiments, and this setup was operated under inert atmosphere achieved by introducing nitrogen (99.996 % N_2) and argon (99.999 % Ar) at flow rates of 12 L/min and 3 L/min, respectively. The temperature was ramped at a rate of 10 K/min to 100 K above the calculated liquidus temperature of each respective slag composition (disregarding the spinel phase in case of primary crystallisation, ie, 100 K above the first crystal to co-precipitate). These calculations were performed using the Equilib module of FactSage 8.2 employing the GTOx database (Bale et al, 2016; Yazhenskikh et al, 2019). The idea of including Cr_2O_3 and subsequently not considering the primary crystallisation of the spinel was accounted for in the previous publication (Andersson et al, 2023b). Based on the calculations, slag A and B were synthesised at 1509 and 1517 K, respectively. After an isothermal section of two hours at the respective temperature, the crucible was removed manually from the furnace, and the slag was granulated in water jets operating with cold tap water at a flow rate of 1.1 L/s. The methodology has been shown to produce synthetic iron silicate slags with relevant and repeatable results (Andersson et al, 2023b).
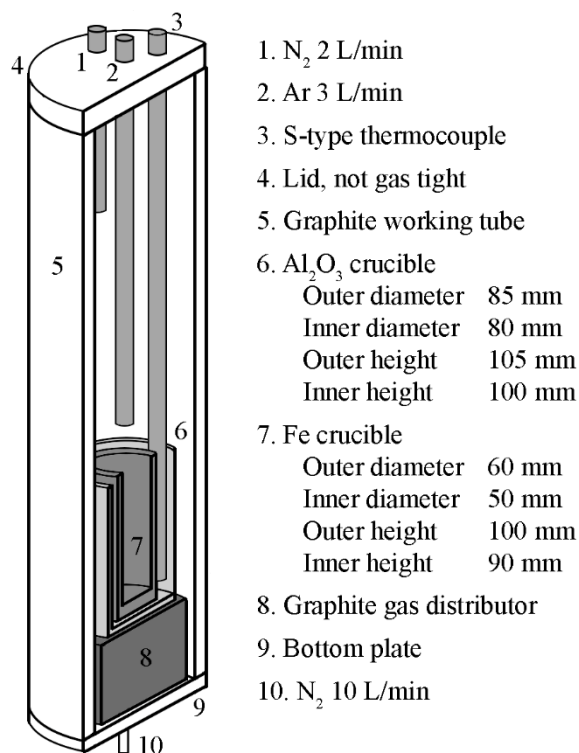
1. N_2 2 L/min

2. Ar 3 L/min

3. S-type thermocouple

4. Lid, not gas tight

5. Graphite working tube

6. Al_2O_3 crucible

Outer diameter	85 mm
Inner diameter	80 mm
Outer height	105 mm
Inner height	100 mm

7. Fe crucible

Outer diameter	60 mm
Inner diameter	50 mm
Outer height	100 mm
Inner height	90 mm

8. Graphite gas distributor

9. Bottom plate

10. N_2 10 L/min

FIG 1 – Schematic overview of the experimental setup.

The synthesised slags were analysed for their chemical composition by an accredited laboratory using inductively coupled plasma mass spectrometry. The digestion of the samples prior to the analyses was achieved via microwave-assisted dissolution in a mixture of hydrochloric acid, nitric acid, and hydrofluoric acid after fusion with lithium metaborate.

Rietveld powder X-ray diffraction (XRD) with an internal standard was used to determine the amorphous content of the two slags. The internal standard calcite (99.5 % $CaCO_3$) was mixed to obtain 10 wt per cent in each sample. Mixing was made using a ring mill, and the subsequent scans were performed between 10 and 90 °2θ with copper K_α generated at 45 kV and 40 mA using a Malvern Panalytical Empyrean X-ray diffractometer (Malvern Panalytical, Malvern, UK). The refinement was performed using HighScore+ and the COD database (Gražulis et al, 2009).

Crystallisation and viscosity

An HT-CLSM (Yonekura VL2000DX-SVF17SP) was utilised to study the crystallisation behaviour of the two slags under continuous cooling experiments. The measurements were performed on sample sizes of 115 mg in molybdenum crucibles. The crucible choice was based on the alloying of platinum with iron experienced for iron silicate slags. Prior to the cooling cycle, the slags were allowed to homogenise at 1673 K for 300 s. The primary crystallisation was determined for the cooling rates of 10, 25, 50, 100, 250, 500, and 1000 K/min.

In accordance with the evaluation of using different crucible and spindle materials for measuring the viscosity of iron silicate slags (Isaksson et al, 2023), the viscosity measurements in the present study were made using the rotating cylinder technique with a spindle and crucible made of molybdenum (tzm molybdenum 364). Details related to the experimental setup, eg, manufacturer, placement of the thermocouple, gas atmosphere, calibration, and control of performance, have been accounted for in a previous publication (Isaksson et al, 2023).

The viscosity was measured at increments of 50 K during a cooling cycle from 1723 to 1423 K. Prior to each measurement at a new temperature, the slag was allowed to homogenise at a constant shear rate until stable values of the viscosity were achieved. The actual measurements were performed at shear rates of 1, 2, 4, 8, and 16 1/s.

Inherent reactivity

The synthetic slags were milled iteratively to a similar specific surface area using a planetary ball mill operated at 600 revolutions per minute with 18 tungsten carbide balls of 10 mm in diameter in 45 mL tungsten carbide grinding bowls. The Brunauer, Emmet, and Teller (BET) specific surface area was measured after degassing at 573 K for 60 min.

The milled samples were subjected to the isothermal calorimetry-based rapid screening test for SCMs outlined by Snellings and Scrivener (2016), further developed and referred to as the rapid, relevant, and reliable (R^3) test by Avet et al (2016). This method was chosen based on the study presented by Li et al (2018), which demonstrated that the R^3 test results correlated strongly with the strength of mortars, independent of the type of SCM and with great repeatability between laboratories. Furthermore, this calorimetry-based testing method tests the inherent reactivity of the SCM without the influence of cement hydration (Hallet, De Belie and Pontikes 2020; Sivakumar et al, 2021). Mixtures were prepared in accordance with Li et al. (2018), and the heat flow was measured for 7 days using a TAM Air isothermal calorimeter. A detailed description of the procedure employed at the current laboratory has been accounted for in a previous publication (Andersson et al, 2023c).

RESULTS AND DISCUSSION

Chemical and mineralogical composition

The analysed chemical compositions of the slags are presented in Figure 2a. For slag A, the FeO and SiO_2 contents were analysed to 53.3 and 38.2 at per cent, respectively. Analogously, for slag B, the FeO and SiO_2 contents were analysed to 61.7 and 30.4 at per cent, respectively. As no volatile components were included in the slags, deviations from the mixed composition should be solely attributed to the possible interaction with the crucible or to analytical errors. Stable oxides such as CaO, Al_2O_3, MgO, and SiO_2 are expected to interact less with the crucible, which is consistent with Figure 2a. More specifically, in comparison to the theoretical or mixed compositions, CaO, Al_2O_3, and MgO were within the experimental error reported by the accredited laboratory. The FeO/SiO_2 ratio of slag B was satisfactory, while slag A deviated from the mixed composition. Additional FeO might enter the slag from oxidation of the ferrous iron to ferric and the subsequent reduction of ferric iron to ferrous iron by the crucible, which could constitute the higher FeO/SiO_2 ratio. However, the experimental setup was operated in an inert atmosphere, which should mitigate the proposed mechanism. Accounting for the reported error in the analysis, the quotient of slag A, determined to be 1.39, is within the experimental error of the theoretical ratio of 1.25. In conclusion, although the FeO/SiO_2 ratio of slag A was analysed to a higher quotient than aimed for, the attained chemical compositions successfully isolated the FeO/SiO_2 ratio as a parameter.
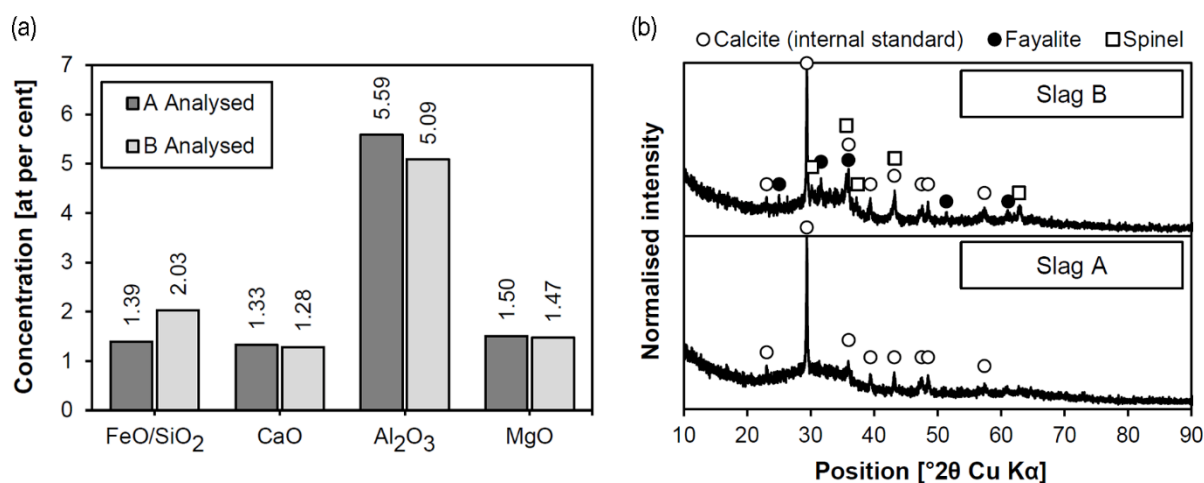

FIG 2 – (a) Chemical compositions in at per cent and quotient of at per cent for the FeO/SiO_2 ratio. (b) X-ray diffractograms of both slags including calcite as internal standard.

The mineralogical compositions of the samples are presented in Figure 2b. Slag A, having a lower FeO/SiO$_2$ ratio, was not analysed for any crystalline phases except the mixed internal standard. Therefore, an entirely amorphous slag was generated. On the other hand, slag B, with an FeO/SiO$_2$ ratio representing stoichiometric fayalite, was analysed for both fayalite and spinel. Based on the Rietveld refinement accounting for the internal standard, slag B was calculated to contain 90.1 wt per cent amorphous slag. Furthermore, spinel and fayalite were determined to constitute 3.3 and 6.6 wt per cent of the sample, respectively.

Crystallisation behaviour and measured viscosities

Based on the equilibrium-type cooling calculations, the liquidus temperatures of slag A and B were estimated to 1553 and 1610 K, respectively. Both slags experienced primary crystallisation of spinel with olivine, ie, fayalite-forsterite solid solution, as the first crystal to co-precipitate. The co-precipitation was calculated to start at 1409 and 1417 K for slag A and B, respectively. Figure 3a presents the results of the HT-CLSM experiments. The dashed lines in the figure represent the continuous cooling temperature curves, and the plotted circles represent the crystallisation, ie, the continuous cooling transformation curves. In comparison to the calculated temperature of primary crystallisation, the slowest cooling rate suggests lower temperatures than those predicted by the GTOx database.
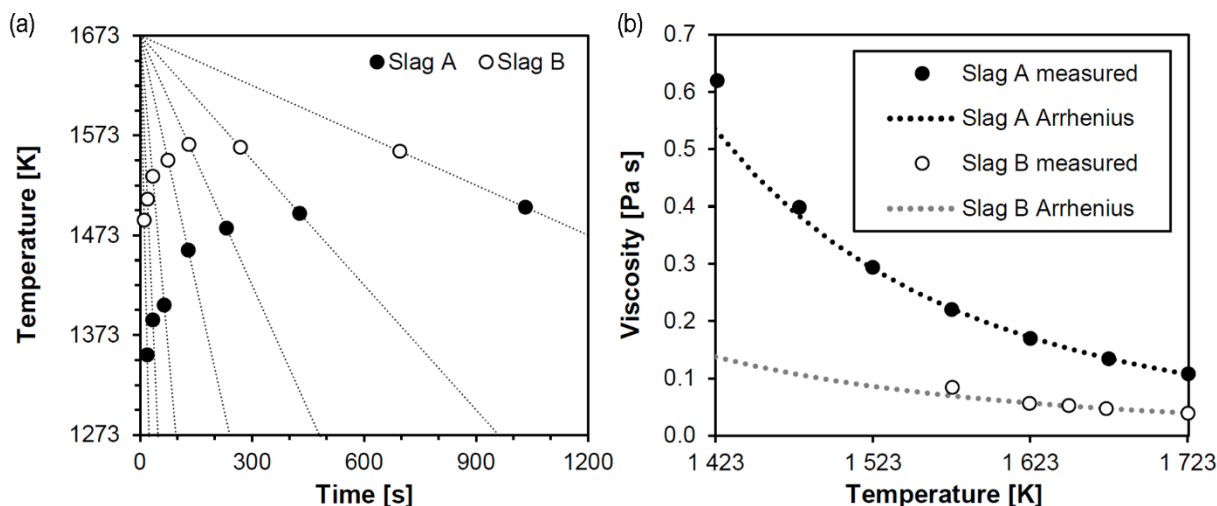

FIG 3 – (a) continuous cooling transformation diagram of the slags. (b) Measured viscosities of the slags.

The juxtaposition of the continuous cooling transformation curves of slag A and B in Figure 3a shows that the former slag is less prone to crystallisation. Both the absolute and relative temperature difference between the crystallisation at 10 K/min and 1000 K/min is more considerable for slag A in comparison to slag B, and, therefore, the granulation of slag A should more easily generate an entirely amorphous material. During the synthesis of the samples, the temperature of onset granulation for slag B (1517 K) was below the temperature of observed primary crystallisation, Figure 3a, which explains the presence of spinel in slag B, Figure 2b. However, in addition to spinel, fayalite was found in slag B, and this observation complies with the data related to the higher tendencies towards crystallisation.

Since low ion migration is related to energy barriers for crystallisation (Deng et al, 2022), the viscosities of slag A and B were measured to indirectly assess the differences in the degree of polymerisation and ion mobility. The average viscosity of 20 measurement points at a shear rate of 8 1/s, at each temperature, is presented as circles in Figure 3b. For slag B, temperatures below 1573 K did not generate consistent values, which indicated that significant crystallisation had occurred. Therefore, the measurements in the cooling cycle were discontinued at 1523 K, and a supplementary measurement at 1648 K was included to incorporate an additional data point in the liquidus region. The viscosity data was used to calculate the activation energy of flow using an Arrhenius-type equation (Equation 1).

$$\eta = Aexp\left(\frac{E_a}{RT}\right)$$
(Equation 1)

where η is the viscosity [Pa s], A is the pre-exponential factor [Pa s], E_a is the activation energy of flow [J/mol], R is the gas constant [J/mol K], and T is the temperature [K]. Since Equation 1 is valid for a fully liquid slag, the calculations of the activation energy of flow were performed for the data points above the liquidus temperature. For slag A, the lowest temperature included in the calculations was 1523 K, which is consistent with the HT-CLSM data presented in Figure 3a. Analogously, for slag B, the calculations were performed with the four data points at 1623 K and above. This approach resulted in activation energies of 109.1 and 84.9 kJ/mol for slag A and B, respectively. Furthermore, the pre-exponential factors were calculated to 53 and 106 µPa s for slag A and B, respectively. The values represent what can be seen in Figure 3b, ie, slag A has higher internal friction of flow. In addition, the activation energies highlight the structural changes with temperature, suggesting that lowering the temperature has higher implications on the structural changes of slag A compared to slag B. Finally, the plotted calculated viscosity for fully liquid slags using the parameters from Equation 1, labelled Arrhenius in Figure 3b, deviates from the measured viscosity in accordance with the crystallisation shown in Figure 3a.

The measured viscosities and the calculated activation energies of flow agree with the degree of polymerisation of the two slags, which can be compared using the ratio between non-bridging oxygen and tetragonally coordinated oxygen (NBO/T) calculated according to the method accounted for in the literature (Mills, 1995). More specifically, the NBO/T was calculated to be 1.92 and 2.91 for slag A and B, respectively, highlighting the network-breaking character of the ferrous oxide. Thus, the data support the observations from the crystallisation experiments and the mineralogical composition after the water granulation. A caveat can be introduced in accordance with the review on the viscosity of glass-forming systems (Zheng and Mauro, 2017), ie, the viscosity-temperature relationship in the fully liquidus state does not necessarily represent the behaviour for a fully liquid supercooled melt. However, as SiO_2 behaves as a strong liquid with Arrhenius behaviour under supercooling while more depolymerised silicate melts are classified as fragile, the viscosity difference of slag A and B during supercooling might be enhanced. In conclusion, generating an entirely amorphous slag during granulation is comparatively more feasible for slag A than for slag B, which is positive for an intended application as an SCM.

Reactivity as a supplementary cementitious material

A previous study on SCMs have shown that the reactivity measured using the R^3 isothermal calorimetry-based experiment correlates to dissolved aluminium and silicon in cement pore solution conditions (Ramanathan et al, 2021). This is consistent with the formation of calcium-silicate-hydrate gel and calcium-aluminium-silicate-hydrate gel, as well as the alumina ferric oxide tri-substituted and mono-substituted phases upon the SCMs consumption of portlandite (Hallet, De Belie, Pontikes, 2020; Sivakumar et al, 2021). In the present study, the iterative milling generated samples with BET specific surface areas of 1.04 and 1.11 m^2/g for slag A and B, respectively. Therefore, the differences in the reactivities measured in the R^3 test, presented in Figure 4, can be attributed to the chemical and mineralogical characteristics of the slags, translating to the dissolution of silicon and aluminium from the slags to the cementitious system.

By depolymerising the slag via the replacement of silica with ferrous oxide, the contribution of silicon per mass unit of dissolved slag is less. Therefore, according to the data presented in Figure 4, slag B has an initially higher dissolution rate, which is consistent with previous studies showing that more depolymerised SCMs have higher dissolution rates in cement pore solution conditions (Snellings, 2013; Schöler et al, 2017).

Despite having an initially higher reaction rate, slag B is less reactive, as seen over the whole experimental period. This observation is still valid if the crystalline content of 9.9 wt per cent is considered inert, ie, if the reactivity in Figure 4 is normalised for the amorphous part of slag B. Dissolving iron into the solution at alkaline pH and redox potentials relevant for cement pore solution conditions has been indicated to be less favourable (Andersson et al, 2023c), which might facilitate the generation of diffusion barriers upon dissolution of the slag. Such a diffusion barrier would be more pronounced for a higher FeO/SiO_2 ratio. Furthermore, depolymerising the slag by replacing silica with ferrous iron oxide lowers the total potential silicon available for the cementitious system. Consequently, the progressively lower heat flow of slag B, generating the intersection observed at 74 h in Figure 4, can be attributed to either mechanism or a combination of both.
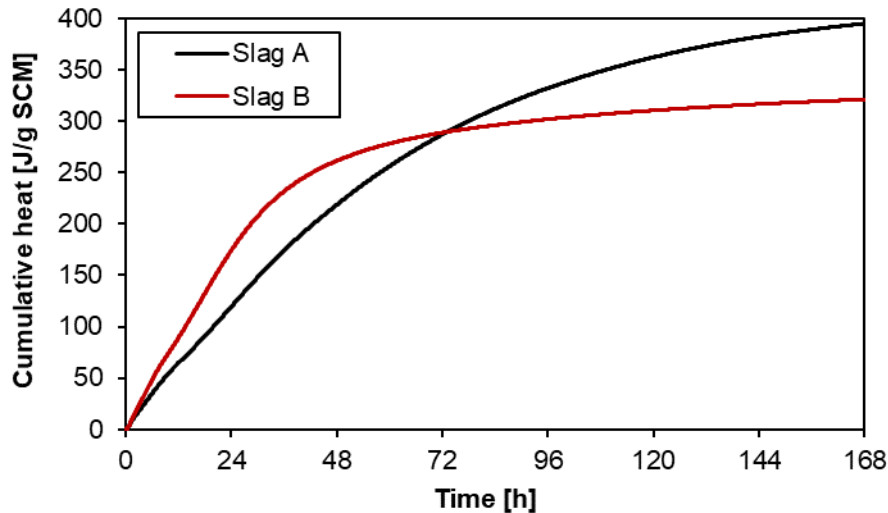
FIG 4 – Cumulative heat from the R^3 isothermal calorimetry experiment.

CONCLUSIONS

In the present study, two synthetic slags within the FeO-SiO_2-CaO-Al_2O_3-MgO-Cr_2O_3 system were studied to isolate the effect of the changed FeO/SiO_2 ratio on the feasibility of utilising the slags as SCMs. Based on the experimental work, the following was concluded:

- By increasing the FeO/SiO_2 ratio from 1.39 to 2.03 (at per cent/at per cent), the viscosity was lowered at comparable temperatures above the liquidus of both slags owing to the network-breaking characteristics of FeO.

- Continuous cooling transformation experiments showed that the slag with higher FeO/SiO_2 ratio had higher inclination towards crystallisation, which corresponds to the mobility within the melt.

- Although the more depolymerised slag had higher initial reactivity as an SCM, the seven-day reactivity was lower, which in combination with the tendency to crystallise suggest that the lower FeO/SiO_2 ratio of the present study is more attractive for slag valorisation as an SCM.

ACKNOWLEDGEMENTS

REFERENCES

Al-Jabri, K S, Taha, R A, Al-Hashmi, A and Al-Harthy, A S, 2006. Effect of copper slag and cement by-pass dust addition on mechanical properties of concrete, *Construction and Building Materials*. 20:322–331.

Andersson, A, Brander, L, Lennartsson, A, Roos, Å and Engström, F, 2023a. Ground Granulated Iron Silicate Slag as Supplementary Cementitious Material: Effect of Prolonged Grinding and Granulation Temperature, *Journal of Cleaner Materials*, 10:100209.

Andersson, A, Brander, L, Lennartsson, A, Roos, Å and Engström, F, 2023b. A method for synthesizing iron silicate slags to evaluate their performance as supplementary cementitious materials, *Applied Sciences*, 13.14:8357.

Andersson, A, Isaksson, J, Lennartsson, A, Engström, F, 2023c. Insights into the valorization of electric arc furnace slags as supplementary cementitious materials, *Journal of Sustainable Metallurgy*, 1-14.

Avet, F, Snellings, R, Diaz, A A, Haha, M B and Scrivener, K, 2016. Development of a New Rapid, Relevant and Reliable (R^3) Test Method to Evaluate the Pozzolanic Reactivity of Calcined Kaolinitic Clays. *Cement and Concrete Research*, 85:1–11.

Bale, C W, Bélisle, E, Chartrand, P, Decterov, S A, Eriksson, G, Gheribi, A E, Hack, K, Jung, I-H, Kang, Y-B, Melançon, J, Pelton, A D, Petersen, S, Robelin, C, Sangster, J, Spencer, P and Van Ende, M-A, 2016. Reprint of: FactSage Thermochemical Software and Databases, 2010–2016, *Calphad*, 55:1–19.

Deng, L, Yao, B, Lu, W, Zhang, M, Li, H, Chen, H, Zhao, M, Du, Y, Zhang, M, Ma, Y and Wang, W, 2022. Effect of SiO_2/Al_2O_3 ratio on the crystallization and heavy metal immobilization of glass ceramics derived from stainless steel slag, *Journal of Non-Crystalline Solids*, 593:121770.

Feng, Y, Kero, J, Yang, Q, Chen, Q, Engström, F, Samuelsson, C and Qi C, 2019a. Mechanical Activation of Granulated Copper Slag and Its Influence on Hydration Heat and Compressive Strength of Blended Cement, *Materials*, 12:772.

Feng, Y, Yang, Q, Chen, Q, Kero, J, Andersson, A, Ahmed, H, Engström, F and Samuelsson, C, 2019b. Characterization and evaluation of the pozzolanic activity of granulated copper slag modified with CaO, *Journal of Cleaner Production*, 232:1112–1120.

Gabasiane, T S, Danha, G, Mamvura, T A, Mashifana, T and Dzinomwa, G, 2021. Environmental and Socioeconomic Impact of Copper Slag—A Review, *Crystals,* 11: 1–16.

Glosser, D, Suraneni, P, Burkan Isgor, O and Jason Weiss, W, 2021. Using glass content to determine the reactivity of fly ash for thermodynamic calculations, *Cement and Concrete Composites*, 115:103849.

Gražulis, S, Chateigner, D, Downs, R T, Yokochi, A F T, Quirós, M, Lutterotti, L, Manakova, E, Butkus, J, Moeck, P and Le Bail, A, 2009. Crystallography Open Database - an Open-Access Collection of Crystal Structures, *Journal of Applied Crystallography*, 42:726–729.

Hallet, V, De Belie, N and Pontikes, Y, 2020. The impact of slag fineness on the reactivity of blended cements with high-volume non-ferrous metallurgy slag. *Construction and Building Materials*, 257:119400.

Isaksson, J, Andersson, A, Lennartsson, A and Samuelsson, C, 2023. Interactions of Crucible Materials With an FeO_x–SiO_2–Al_2O_3 Melt and Their Influence on Viscosity Measurements, *Metallurgical and Materials Transactions B*, 54B:3526-3541.

Kero Andertun, J, Samuelsson, C, Peltola, P and Engström, F, 2022. Characterisation and leaching behaviour of granulated iron silicate slag constituents, *Canadian Metallurgical Quarterly*, 61:14–23.

Kucharczyk, S, Sitarz, M, Zajac, M and Deja, J, 2018. The effect of CaO/SiO_2 molar ratio of $CaO-Al_2O_3-SiO_2$ glasses on their structure and reactivity in alkali activated system, *Spectrochimica Acta Part A: Molecular and Biomolecular Spectroscopy,* 194:163–171.

Li, X, Snellings, R, Antoni, M, Alderete, N M, Haha, M B, Bishnoi, S, Cizer, Ö, Cyr, M, De Weerdt, K, Dhandapani, Y, Duchesne, J, Haufe, J, Hooton, D, Juenger, M, Kamali-Bernard, S, Kramar, S, Marroccoli, M, Joseph, A M, Parashar, A, Patapy, C, Provis, J L, Sabio, S, Santhanam, M, Steger, L, Sui, T, Relesca, A, Vollpracht, A, Vargas, F, Walkley, B, Winnefeld, F, Ye, G, Zajac, M, Zhang, S and Scrivener K L, 2018. Reactivity Tests for Supplementary Cementitious Materials: RILEM TC 267-TRM Phase 1, *Materials and Structures*, 51:151.

Lothenbach, B, Scrivener, K and Hooton, R D, 2011. Supplementary cementitious materials, *Cement and Concrete Research*, 41:1244–1256.

Mills, K C, 1995. Structure of liquid slags, in *Slag atlas* (ed: D Springorum), pp 1–8 (Verlag Stahleisen GmbH: Düsseldorf).

Murari, K, Siddique, R and Jain, K K, 2015. Use of waste copper slag, a sustainable material, *Journal of Material Cycles and Waste Management*, 17:13–26.

Ramanathan, S, Perumal, P, Illikainen, M, Suraneni, P, 2021. Mechanically activated mine tailings for use as supplementary cementitious materials, *RILEM Technical Letters*, 6:61–69.

Ramanathan, S, Tuen, M and Suraneni, P 2022. Influence of supplementary cementitious material and filler fineness on their reactivity in model systems and cementitious pastes, *Materials and Structures*, 55.5:136.

Romero Sarcos, N, Hart, D, Bornhöft, H, Ehrenberg, A and Deubener, J, 2021. Rejuvenation of granulated blast furnace slag (GBS) glass by ball milling, *Journal of Non-Crystalline Solids*, 556:120557.

Schöler, A, Winnefeld, F, Haha, M B and Lothenbach, B, 2017. The effect of glass composition on the reactivity of synthetic glasses. *Journal of the American Ceramic Society*, 100.6:2553-2567.

Shi, C, Meyer, C and Behnood, A, 2008. Utilization of copper slag in cement and concrete, *Resources, Conservation and Recycling,* 52:1115–1120.

Sivakumar, P P, Matthys, S, De Belie, N, and Gruyaert, E, 2021. Reactivity assessment of modified ferro silicate slag by R^3 method, *Applied Sciences*, 11.1:366.

Skibsted, J and Snellings, R, 2019. Reactivity of supplementary cementitious materials (SCMs) in cement blends, *Cement and Concrete Research*, 124:105799.

Snellings, R, 2013. Solution-controlled dissolution of supplementary cementitious material glasses at pH 13: the effect of solution composition on glass dissolution rates. *Journal of the American Ceramic Society*, 96.8:2467-2475.

Snellings, R and Scrivener, K L, 2016. Rapid Screening Tests for Supplementary Cementitious Materials: Past and Future. *Materials and Structures*, 49:3265–3279.

Stebbins, J F, 1988. Effects of temperature and composition on silicate glass structure and dynamics: Si-29 NMR results, *Journal of Non-Crystalline Solids*, 106:359–369.

Yazhenskikh, E, Jantzen, T, Hack, K and Müller, M, 2019. A New Multipurpose Thermodynamic Database for Oxide Systems, *Rasplawy,* 2:116–124.

Zhang, Q, Deng, D, Feng, Y, Wang, D, Liu, B and Chen, Q, 2023. Effect of Al_2O_3 on the Structural Properties of Water-Quenched Copper Slag Related to Pozzolanic Activity, *Minerals*, 13.2:174.

Zheng, Q and Mauro, J C, 2017. Viscosity of glass-forming systems, *Journal of the American Ceramic Society*, 100.1:6-25.